Journal Name

ARTICLE

The dietary flavonoid eupatilin attenuates *in vitro* lipid peroxidation and targets lipid profile in cancer HeLa cells

Received 00th January 20xx,
Accepted 00th January 20xx

DOI: 10.1039/x0xx00000x

www.rsc.org/

A. Rosa,[*a] R. Isola[a], F. Pollastro[b], P. Caria[a], G. Appendino,[b] and M. Nieddu[a]

Eupatilin is a dietary flavonoid isolated from the alpine wormwoods, used for the genepy liqueur production. This flavone protects cells and tissues towards oxidative stress and targets cancer cells, inducing cytotoxicity, cell circle arrest, apoptosis and mitochondrial dysfunction. This study examines the EUP *in vitro* antioxidant effects on cholesterol and phospholipid membrane oxidation and explores its ability to modulate cancer cell lipid profile. This flavone remarkably protected fatty acids and cholesterol against oxidative degradation by scavenging lipoperoxyl radicals. EUP (24 h of incubation) significantly reduced viability and modulated the total lipid and fatty acid profiles in cancer Hela cells. It induced marked changes in the phospholipid/cholesterol ratio, significant decreases in the levels of oleic and palmitic acids and a marked increase of stearic acid, involving an inhibitory effect on de novo lipogenesis and desaturation in cancer cells. Moreover, a noteworthy mitochondrial membrane depolarization, signs of apoptosis, abnormal mitosis with multi-nucleation (mitotic catastrophe) and morphological alterations were observed in cancer EUP-treated cells. Our results validate the EUP role as antioxidant agent for the treatment/prevention of disorders implicating a membrane lipid oxidative damage and substantiate cell lipid metabolism as another possible target of this dietary natural flavonoid in cancer HeLa cells.

Eupatilin (5,7-dihydroxy-3',4',6-trimethoxyflavone) (EUP) (Fig. 1) is a pharmacologically active *O*-methylated flavone identified in many plants of *Centaurea*, *Salvia*, and *Tanacetum* species,[1,2] and it is the major active component of *Artemisia asiatica* Nakai and *Artemisia princeps* Pampanini, herbs with traditional applications in medicines, spices, teas, or as a cooking ingredient.[3] Regarding the *Artemisia* genus, EUP is specially found in the commonly known génépi plant groups[1,4,5] in which it represents the major lipophilic flavonoid of *Artemisia umbelliformis* Lam. and *Artemisia genipi* Weber, the mountain wormwoods used for the production of the popular alpine liqueur genepy.[4,6] Previous studies have reported that EUP has a wide range of biological activities, including anti-inflammatory,[1,4,7,8] immune regulation,[9] cardioprotective,[10] anti-allergic,[11] anti-adipogenic,[12] neuroprotective,[1,13] antioxidant,[1,8,14-18] and antitumor[1,5,19,20] properties, and represents the active compound in the Korean Stillen®, a natural remedy widely used to treat gastritis and peptic ulcers.[21]

It seems well established that EUP, like other flavonoids,[22] has both *in vitro* and *in vivo* antioxidant properties.[1] In fact, this dietary flavone was found to inhibit ROS production and cellular oxidative stress in ARPE-19 cells[15] and THP-Ms activate macrophages,[8] and to protect AGS gastric epithelial cells against H_2O_2- and $FeSO_4$-induced cell injury in a dose-dependent manner, down-regulating also genes responsible for the cellular oxidative stress.[14] The radical scavenging properties of EUP with the hydroxyl radical ($OH^{\bullet}$) in solution has been correlated to the hydrogen abstraction process, governed by proton coupled electron transfer mechanism.[17] Despite EUP has been proposed to be used as an antioxidant agent for the treatment of ROS-mediated diseases,[13,14,16] there is a lack of information about its antioxidant activity in terms of direct antioxidant protection against ROS production.[14,17,18]

Evidences showed that EUP has *in vitro* and *in vivo* anticancer properties, modulating a variety of molecular targets in order to inhibit cancer cell viability, proliferation, migration, and invasion, showing synergetic effects on cell cycle arrest, cytoskeletal organization, apoptosis, mitochondria membrane potential reduction and numerous cell signaling

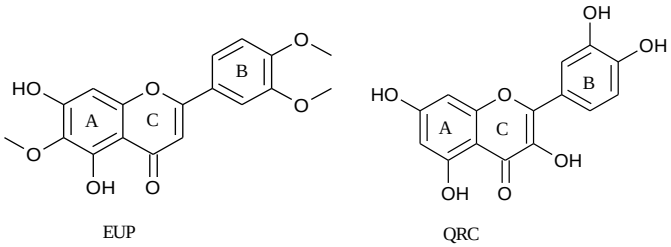

Fig. 1 Chemical structures of eupatilin (EUP) and quercetin (QRC).

[a] *Department of Biomedical Sciences, University of Cagliari, Cittadella Universitaria, Km 4.5 SS 554, 09042 Monserrato (CA), Italy. E-mail: anrosa@unica.it; Fax: ++39/070/6754032; Tel: ++39/070/6754124;*
[b] *Department of Pharmaceutical Sciences, University of Eastern Piedmont, Largo Donegani 2, 28100 Novara, Italy.*

pathways in distinct cancer types.[1,3,5,19,20,23,24] Moreover, the anticancer activity of EUP has been reported to be also mediated through its pro-antioxidant activity.[1,20] Recent studies showed that lipid metabolism could be considered as a promising anticancer target.[25-27] Indeed, several antitumor drugs (lipophilic or amphiphilic molecules) act through the membranes by changing the general lipid membrane organization and structure[28] and many natural compounds exert their anticancer activity by inhibiting the expression of enzymes involved in lipid metabolism like fatty acid synthase[26,29] and stearoyl-CoA desaturase.[26,30] In cancer cells, changes in lipid components severely alter membrane fluidity and protein dynamics, seriously affecting functional and biophysical properties of cytoplasmic and organelle membranes, perturbing membrane lipid rafts, and inducing apoptotic pathways eventually resulting in cell death.[25,26] EUP has been indicated as a potential therapeutic and chemopreventive agent for the treatment of different types of cancer,[1,20,24] however, to the best of our knowledge, no previous study has evidenced the possible modulatory effect of EUP on lipid components in cancer cells.

Thus, starting from all these considerations, in this manuscript we investigated the direct EUP ability to prevent lipid peroxidation in oxidative stress systems of biological relevance like the oxidative damage to cholesterol and phospholipids, essential components of biological membranes and lipoproteins. Oxidation of lipids components is well known to play a role in the development of tissue damage associated with several diseases, including cancer.[31,32] Moreover, experiments were designed to evidence another possible mechanism of EUP in terms of ability to affect cell lipid profile in cancer cells, with regard to the total fatty acid composition, cytoplasmic membranes, phospholipids (PL) and free cholesterol (FC) levels. Changes in lipid profile was analyzed in EUP-treated cancer cells together with the investigation of the cell growth, the apoptosis appearance and the changes occurring on cytoplasmic membranes, nuclear morphology and mitochondria membrane potential.

2. Materials and Methods

2.1. Materials

Cholesterol, 5-cholesten-3β-ol-7-one (7-keto), 5-cholestene-3β,7β-diol (7β-OH), quercetin, standards of fatty acids, 1,2-dipalmitoyl-sn-glycero-3-phosphocholine (PC 16:0/16:0), 1,2-dioleoyl-sn-glycero-3-phosphocholine (PC 18:1/18:1), 1-palmitoyl-2-oleoyl-sn-glycero-3-phosphocholine (PC 16:0/18:1), 1-oleoyl-2-palmitoyl-sn-glycero-3-phosphocholine (PC 18:1/16:0), 2-linoleoyl-1-palmitoyl-sn-glycero-3-phosphocholine (PC 16:0/18:2), 2-arachidonoyl-1-palmitoyl-sn-glycero-3-phosphocholine (PC 16:0/20:4), 1,2-dilinoleoyl-sn-glycero-3-phosphocholine (PC 18:2/18:2), 1,2-dieicosapentaenoyl-sn-glycero-3-phosphocholine (PC 20:5/20:5), 3-(4,5-dimethylthiazol-2-yl)-2,5-diphenyltetrazolium bromide (MTT), the mixture of phospholipids (bovine brain extract, Type VII, purity > 99%), API (4',6-diamidino-2-phenylindole), Nile Red (9-diethylamino-5H-benzo[a]phenoxazine-5-one) and all solvents used, of the highest available purity (≥99.9%), were obtained from Sigma-Aldrich (Milan, Italy). Tetramethylrhodamine methyl ester perchlorate (TMRM) was purchased from Molecular Probes (Eugene, OR, USA). Cell culture materials, Alexa Fluor 488 Annexin V and Propidium Iodide (PI) staining were purchased from Invitrogen, Life Technologies (Milan, Italy). All the chemicals used in this study were of analytical grade. EUP has been isolated from the Swiss chemotype of *A. umbelliformis* Lam. (Asteraceae) as previously reported.[33]

2.2. Cholesterol oxidation assay

The protective effect of aliquots (1-50 nmol) of EUP was evaluated during the cholesterol oxidation in dry state as previously reported.[34] Aliquots of 0.5 ml of cholesterol solution (2 mg/mL of methanol) were dried in a round-bottom test tube under vacuum and then incubated in a bath at 140 °C for 1 h (oxidized controls) under artificial light exposure; controls (Ctrl, non-oxidized cholesterol) were kept at 0 °C in the dark. In a different set of experiments, aliquots of EUP (0.5 mg/ml in methanol) solutions were added to the cholesterol solution, the mixtures cholesterol/flavonoid were dried under vacuum and then incubated for 1 h in dry state in a bath at 140 °C. HPLC-DAD analyses of cholesterol, 7-ketocholesterol (7-keto), and 7β-hydroxycholesterol (7β-OH) were carried out as previously described.[34] The protective effect of aliquots (1-50 nmol) of the reference flavonoid quercetin (QRC) (1 mg/ml in methanol) was also tested in the same experimental conditions as comparison.

2.3. Liposomes oxidation assay

Phospholipids (PL; bovine brain extract) were dissolved in chloroform to obtain 1 mg/mL stock solution. Aliquots (300 μL) of PL solution were dried in a round-bottom test tube under vacuum alone or in the presence of different aliquots of EUP and the reference compound QRC (10, 25 and 50 μM, in methanol solution). After solvent evaporation under vacuum, the thin lipid films were hydrated with saline solution (1 mg/mL solution) and the liposome dispersions (corresponding to 300 μg of lipids) were oxidized in saline solution for 24 h in the presence of 5 μM $CuSO_4$ at 37 °C in a thermostatic water bath as previously reported.[34] Preparation of fatty acids (FA) was obtained by mild saponification.[34] Analyses of unsaturated FA (UFA) were carried out with an Agilent Technologies 1100 liquid chromatograph (HPLC) equipped with a diode array (DAD) detector with a mobile phase of $CH_3CN/H_2O/CH_3COOH$ (75/25/0.12, v/v/v), at a flow rate of 2.3 mL/min, and data were collected and analyzed using the Agilent OpenLAB Chromatography data system, as previously described.[34]

2.4. Cell Culture

Human carcinoma HeLa cell line was obtained from the American Type Culture Collection (ATCC, Rockville, MD). Cells were grown in Dulbecco's modified Eagle's medium (DMEM), supplemented with 10% fetal calf serum (FCS), penicillin (100

units/mL)–streptomycin (100 μg/mL), and 2 mM L-glutamine in a 5% CO_2 incubator at 37 °C. Subcultures of the HeLa cells were grown in T-75 culture flasks and passaged with a trypsin-EDTA solution.

2.5. Cytotoxic activity in cancer cells: MTT assay

The cytotoxic effect of EUP was evaluated in cancer HeLa cells by the MTT assay.[35] Cancer cells were seeded in 96-well plates (density of 3×10^4 cells/mL) in 100 μL of medium and cultured for 48 h. Cells were subsequently incubated for 24 h with various concentrations (0.5-200 μM, dissolved in DMSO) of EUP in complete culture medium (treated cells). Treated cells were compared for viability to untreated cells (control cells) and vehicle-treated cells (incubated for 24 h with an equivalent volume of DMSO; maximal final concentration, 2%). At the end of the incubation time, cells were subjected to the MTT test as previously reported.[35] The cytotoxicity of different concentrations of the anticancer compound QRC (from 0.25 to 200 μM, in DMSO solution) was also tested for 24 h in HeLa cells for comparison. Preliminary evaluation of the cancer cell morphology after 24 h of incubation with various amounts of EUP was performed by microscopic analysis with a ZOE™ Fluorescent Cell Imager (Bio-Rad Laboratories, Inc., California, USA).

2.6. Lipid profile modulation in HeLa cells

For lipid profile modulation experiments, cancer HeLa cells were plated in Petri dishes at a density of about 10^6 cells/10 mL of complete medium as previously reported.[36] Cells were subsequently incubated (at 80% confluence) for 24 h with EUP (10, 25 and 50 μM, in DMSO solution) in complete culture medium (treated cells). Untreated cells (control cells) and vehicle-treated cells (24 h-incubation with 0.5% of DMSO) were also prepared. Cells were scraped after treatment, washed (to remove dead cells), and centrifuged (at 1200 *g* at 4 °C for 5 min), and the pellets, separated from the supernatants, were used for the extraction and analyses of cell lipids.

2.7. HeLa cancer cell lipid extraction and analysis

Total lipids were extracted from HeLa cell pellets using the mixture $CHCl_3$/MeOH/H_2O 2:1:1 as previously reported.[35] Dried aliquot of the $CHCl_3$ fraction, from each cell sample, was dissolved in MeOH and injected into the HPLC system for the direct analysis of phospholipids (PL) and free cholesterol (FC). Another aliquot of dried $CHCl_3$ fractions, dissolved in EtOH, was subjected to mild saponification[35] for the analysis of cell FA. Analyses of lipid compounds were carried out with an Agilent Technologies 1100 HPLC equipped with a DAD and an Agilent Technologies Infinity 1260 evaporative light scattering detector (ELSD). Analyses of unsaturated (DAD detection, 200 nm) and saturated (ELSD detection) FA, obtained from cell lipid saponification, were carried out as previously reported.[35,37] An Inertsil ODS-2 column (Superchrom, Milan, Italy), with MeOH as the mobile phase, at a flow rate of 2 mL/min and ELSD detection, was also used for the direct analyses of PL and FC in lipids extracted from HeLa cells.[35,37] FC in cell lipid extracts was determined by HPLC-DAD quantification at 203 nm with MeOH as the mobile phase, at a flow rate of 0.7 mL/min.[37] Recording and integration of the chromatogram data were carried out through an Agilent OpenLAB Chromatography data system. The identification of lipid components was performed using standard compounds and conventional UV spectra. Calibration curves of FA were constructed using standards and were found to be linear (DAD) and quadratic (ELSD) (correlation coefficients > 0.995).[37]

2.8. Apoptosis assay

Microscopy and flow cytometry analyses were used in order to investigate the EUP-induced apoptosis in cancer cells. Briefly, for immunofluorescent experiments, HeLa cells (density of 10^5 cells/mL) were seeded in 6/well plates (Corning, USA) in 2 ml of complete medium and cultured for 48 h. Then, cells were treated with various concentrations (10, 25 and 50 μM) of EUP (treated cells) and incubated for 24 h in complete medium. Treated and untreated cells were evaluated by Alexa Fluor 488 Annexin V and Propidium Iodide (PI) staining (Invitrogen, Life Technologies, Italy), according to the manufacturer's instructions. The cells were observed with the ZOE™ Fluorescent Cell Imager using filters for fluorescein (FITC) and Texas Red (excitation at 480/17 nm and 556/20 nm, respectively).

Apoptosis was also evaluated by flow cytometry. HeLa cells were seeded in 6-well plates at the density of 10^5 cells/mL. Cells were then treated with different concentrations of EUP (10, 25 and 50 μM) for 24 h. The cells were detached, washed once with PBS 1X and re-suspended in 100 μL of Annexin binding buffer plus of Annexin V-FITC and PI, according to the manufacturer's instructions. Stained cells were then analyzed by flow cytometry, measuring the fluorescence emission at 530 and 620 nm using 488 nm excitation laser (MoFloAstrios EQ, Beckman Coulter). Cell apoptosis was analyzed using Software Summit Version 6.3.1.1, Beckman Coulter.

2.9. Fluorescence microscopy

For fluorescent microscopy studies cells were seeded in 35 mm Petri dishes and treated with 10, 25 or 50 μM EUP or not (control) when they reached 80% confluence. Twenty-four hours after treatment cells were stained with 300 nM Nile Red (NR) or 50 μM TMRM plus 10 μg/mL DAPI in DMEM without serum in a CO_2 incubator for 45 min. Prior observation, dyes were washed out from petri dishes in order to avoid background fluorescence. HeLa cells were observed under a Zeiss Axioskop upright fluorescence microscope (Zeiss, Jena, Germany), equipped with 10x, 20x and 40x/0.75 NA water immersion objectives. NR red fluorescence, corresponding to cytoplasmic membranes,[37] and TMRM fluorescence, indicating mitochondrial potential,[38-39] were acquired with 546±6 excitation filter and 620±60 emission filter. DAPI nuclear fluorescence was observed with 360±20 excitation filter, and 460±25 emission filter. Fluorescence images were acquired

with a cooled CCD camera (QICAM, Qimaging, Canada). Image analysis of TMRM images was performed with Image J and Image Pro Plus (Media Cybernetics, Silver Springs, MD). Briefly, background fluorescence was subtracted from images and histogram values of fluorescence intensity were normalized per cell number. Per each EUP dose and control samples 5-6 images, acquired with an objective 20x (embracing 20-80 cells each), were processed for image analysis.

2.10. Statistical analysis

Graph Pad INSTAT software (GraphPad software, San Diego, CA) was used to calculate the means and standard deviations of two, three or four independent experiments involving triplicate analyses for each sample. Evaluation of the statistical significance of differences was performed using one-way analysis of variation (One-way ANOVA), and the Bonferroni post Test. Results were expressed as mean ± standard deviation (SD), and statistically significant differences was evaluated with $p < 0.05$ as a minimal level of significance.

3. Results

3.1. Protective effect against cholesterol oxidation

The antioxidant activity of EUP was assessed during cholesterol oxidation in dry state.[34,40] Quercetin (QRC) (Fig. 1), the well-known bioactive dietary flavonoid, was also tested in the same model as reference antioxidant compound. Aliquots of dried cholesterol were incubated for 1 h alone (oxidized control) or in the presence of different amounts of flavonoids. The decrease of the cholesterol level (at 140 °C, cholesterol was an oil) and its transformation in its oxidized products (7-keto and 7β-OH) was measured as marker of the oxidative process. Fig. 2A shows the antioxidant activity, expressed as % protection, of different amounts (1-50 nmol) of EUP measured during cholesterol degradation. Values (μg) of oxysterols (7β-OH and 7-keto) measured in the control (Ctrl, at 0 °C) and in the absence (0, oxidized control) and in the presence of EUP are also reported in Fig. 2C. In this system EUP exerted a significant 49% protection of cholesterol at 10 nmol, showing > 80% protection from 25 nmol. Contemporaneously, EUP exerted a significant reduction of the 7-keto formation with respect to oxidized control from 10 nmol, also decreasing the 7β-OH generation. QRC showed a significant 70% protection at 2.5 nmol and a complete inhibition (90-100%) of the oxidative process from 10 nmol (Fig. 2B), significantly preventing the formation of 7-keto from 2.5 nmol and 7β-OH from 25 nmol (Fig. 2D). The value (nmol) of the amount of EUP (IA_{50}) that gives a protection of 50% of the cholesterol decrease during 1 h oxidation is reported in Table 1, together with values obtained for a series of natural phenolic antioxidants previously tested in similar experimental conditions.[34,37,40,41] Although in this test EUP was less potent than the phenolic compounds QRC (IA_{50} 1.8 nmol), curcumin[40] and homogentisic acid,[41] it still exerted an interesting antioxidant activity (IA_{50} of 10.5 nmol) in protecting sterol against the oxidative degradation, comparable to that of the bioactive phenolic compounds arzanol, methylarzanol[34] and prenylcurcumin.[40]

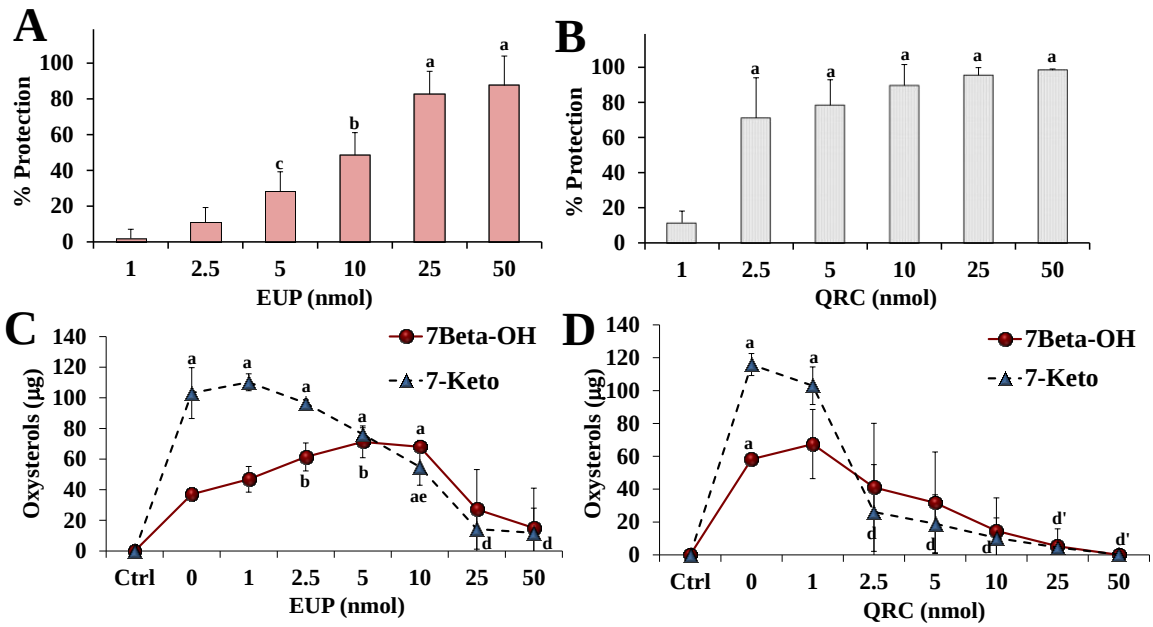

Fig. 2 Antioxidant activity, expressed as % protection, of different amounts (1-50 nmol) of eupatilin (EUP) (A) and the reference flavonoid quercetin (QRC) (B) measured during cholesterol oxidation at 140 °C for 1 h, a = $p < 0.001$, b = $p < 0.01$, c = $p < 0.05$, versus oxidized control (0% protection). Values (μg) of oxysterols (7β-OH and 7-keto) measured in the control (Ctrl) and in the absence (0, oxidized control) and in the presence of different aliquots (1-50 nmol) of EUP (C), and QRC (D), during cholesterol oxidation at 140 °C for 1 h, a = $p < 0.001$, b = $p < 0.01$ versus Ctrl, d = $p < 0.001$, d' = $p < 0.001$ for both oxysterols, e = $p < 0.01$, versus oxidized control (0). Three independent experiments are performed, and data are presented as mean ± SD (n = 6).

3.2 Protective effect against liposome oxidation

The protective effect of EUP was then evaluated versus the liposome oxidative injury. The chromatographic profile of unsaturated FA (UFA) of control liposomes by HPLC-DAD is shown in Fig. 3A. The values of the main UFA in control liposome (0 °C) were: oleic acid 18:1 n-9, 99.1 ± 11.1 μg; arachidonic acid 20:4 n-6, 18.6 ± 1.3 μg; docosatetraenoic acid 22:4 n-6, 19.8 ± 1.8 μg; docosahexaenoic acid 22:6 n-3, 27.0 ± 1.2 μg/mg liposomes. Liposomes were treated with Cu^{2+} ions for 24 h and the variation of UFA concentrations was analyzed as an index of the lipid peroxidation process. Figs. 3B and 3C show total values of the main polyunsaturated FA (20:4 n-6, 22:4 n-6, 22:6 n-3) (PUFA) (expressed as % of the control) measured in the control (Ctrl) and during liposome oxidation in the absence (0, oxidized control) and in the presence of different concentrations (10, 25 and 50 μM) of EUP (Fig. 3B) and the reference phenol QRC (Fig. 3C). A strong and significant decrease (40%) of PUFA level was observed at 24 h oxidation in oxidized control. EUP showed a significant antioxidant activity against PUFA consumption at all tested concentrations, with a protection of 36, 50 and 64% at 10, 25 and 50 μM, respectively. At 10 μM, this flavone was less active than QRC (92% protection), arzanol (89%)[34] and curcumin (71%),[40] nonetheless showed an antioxidant potency comparable to that of methylarzanol,[34] as shown in Table 1.

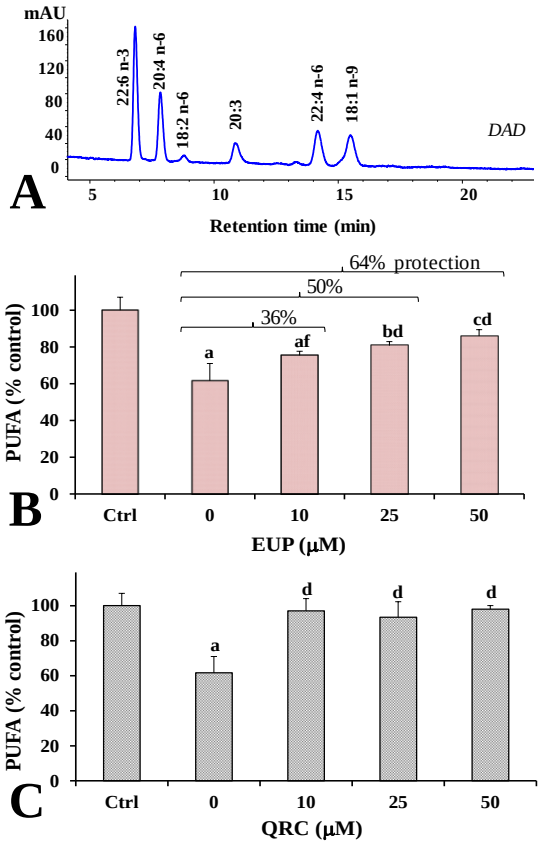

Fig. 3 Chromatographic profile, obtained by HPLC-DAD analysis, of unsaturated fatty acids measured in control liposomes (A). Total values of polyunsaturated fatty acids (PUFA), expressed as % control, measured in control liposomes (Ctrl) and during liposome oxidation at 37 °C for 24 h with 5 μM $CuSO_4$ in the absence (oxidized control, 0) or in the presence of different amounts (10, 25, 50 μM) of eupatilin (EUP) (B) and quercetin (QRC) (C). The % protection of EUP on PUFA consumption is reported for each concentration. Three independent experiments are performed, and data are presented as mean ± SD (n = 6), a = $p < 0.001$, b = $p < 0.01$, c = $p < 0.05$, versus Ctrl, d = $p < 0.001$, f = $p < 0.05$ versus 0.

Table 1 Antioxidant activity of eupatilin (EUP) and reference compounds[34,37,40,41] during cholesterol oxidation at 1 h in dry state, calculated as IA_{50} values (amount that gives a protection of 50%, expressed as nmol) and during Cu^{2+}-induced liposome oxidation at 37 °C for 24 h, measured as % protection at 10 μM.

Compounds	IA_{50} values (nmol, at 1 h)	% Protection (10 μM)
Arzanol[34]	5.6	89.1
Curcumin[40]	< 1	71.5
EUP	10.5	36.0
Homogentisic acid[41]	1.1	15.0
Methylarzanol[34]	7.1	31.7
Prenylcurcumin[40]	5.5	65.6
QRC	1.8	92.2
Zerumbone[37]	NA	NA

3.3. Cytotoxic activity on HeLa cells

The cytotoxic effect of EUP was investigated on cancer HeLa cells. Fig. 4A shows the viability, expressed as % of the control, induced by incubation for 24 h with different amounts (0.5-200 μM) of EUP and the reference compound QRC in cancer HeLa cells by MTT assay. EUP was not significantly toxic at the dose

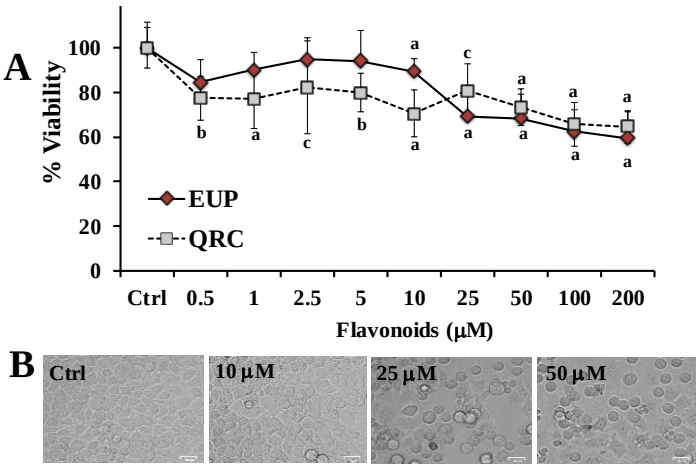

Fig. 4 (A) Viability, expressed as % of the control (Ctrl), induced by incubation for 24 h with different amounts (0.5-200 μM) of eupatilin (EUP) and the reference compound quercetin (QRC) in cancer HeLa cells (MTT assay). Three independent experiments are performed, and data are presented as mean ± SD (n = 12), a = $p < 0.001$, b = $p < 0.01$, c = $p < 0.05$ versus Ctrl. (B) The panel shows representative images of phase contrast of control HeLa cells (Ctrl) and cells treated for 24 h with EUP 10, 25 and 50 μM. Bar = 30 μm

range of 0.5-5 μM, whereas exerted a significant reduction in HeLa cell viability, in comparison with control cells, from the dose of 10 μM (low reduction of viability, 11%). A significant marked reduction of viability, ranging from 31 to 41%, was observed from the dose of 25 μM to 200 μM. The treatment with QRC induced a statistically significant decrease in cancer cell viability, with respect to control, from the concentration of 0.5 μM (22% of reduction), and similar values were observed in the dose range 1-50 μM, with a viability reduction of 34 and 36% at 100 and 200 μM, respectively. DMSO, used to dissolve the flavonoids, was not toxic in HeLa cancer cells and cell viability, measured at the maximal tested dose (2%), was 92%. It was not possible to determine the exact IC_{50} (the concentration that decreases the cell viability to 50%) value for EUP in HeLa cells at 24 h incubation, because under the used experimental conditions, this value exceeds the solubility of the compound and the maximum tolerated DMSO percentage (2%) in cell cultures. The preliminary microscopic observation of EUP-treated cells before MTT assay, allowed us to evidence different cell morphologies in HeLa cells after 24 h-incubation at the different doses. The panel B in Fig. 4 shows representative images of phase contrast of control HeLa cells and cells treated for 24 h with EUP 10 μM (89% of viability, normal cell morphology), 25 μM (69% of viability, cells with apoptotic morphology) and 50 μM (67% of viability, apoptotic morphology of most cells), concentrations that have been chosen for further experiments.

3.4. Effect on cell lipid components

EUP was then tested in cancer HeLa cells to assess its effects after 24 h-incubation on cancer cell lipid composition at different levels of toxicity. The EUP effect on cell polar lipid classes and total FA (TFA) profile was evaluated. Figure 5A shows the chromatographic profile of lipid compounds of HeLa control cells and cells treated for 24 h with EUP 10, 25, and 50 μM obtained by HPLC-ELSD analysis. The chromatographic region for each lipid class was assigned by using standard mixtures of saturated, monounsaturated (S/M-PL) and polyunsaturated (P-PL) phosphatidylcholines, and free cholesterol (FC). Cell polar lipids (phospholipids, PL; FC) were separated from neutral lipids that eluted at higher retention times.[36,37] The reversed phase mode used allowed to separate lipid components on the basis of ECN (=CN−2n, where CN is the number of acyl group carbons and n the number of double bonds) and lipids containing FA with the same ECN co-eluted.[36,37] In our experimental conditions, control HeLa cells showed a polar lipid profile characterized by a peak of FC and two main peaks of PL, corresponding to saturated/monounsaturated PL (S/M-PL) and polyunsaturated PL (P-PL). EUP-treated cells (10, 25 and 100 μM) showed a marked change in the lipid profile, with a marked significant decrease in the peak areas of S/M-PL ($p < 0.001$ versus untreated cells) and an increase in the % of FC ($p < 0.001$ versus untreated cells from 25 μM), coupled to a slight decrease in P-PL% (Fig. 5B). By HPLC, the FC level was measured in HeLa control cells as a mean content of 102.6 ± 8.9 μg per plate, with a total FA (TFA)/FC ratio value of 3.4 ± 1.2. The 24 h-incubation with EUP induced in treated cells a reduction in the TFA/FC ratio, with a value of 2.8 ± 0.1 ($p < 0.05$ versus untreated cells) at EUP 50 μM, due to a

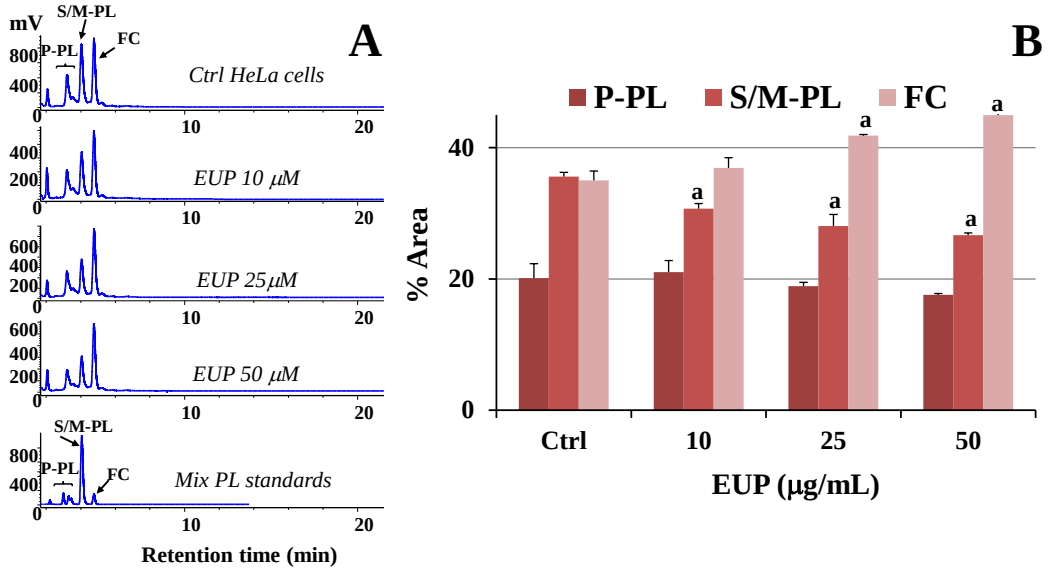

Fig. 5 Chromatographic profile, obtained by HPLC-ELSD analysis at 2 mL/min, of saturated/monounsaturated phospholipids (S/M–PL), polyunsaturated phospholipids (P-PL) and free cholesterol (FC), measured in control HeLa cells (Ctrl) and cells treated for 24 h with different amounts (10, 25 and 50 μM) of eupatilin (EUP) (A). The chromatographic region for each lipid class was assigned by using standard mixtures of saturated/monounsaturated (mix PL: PC 16:0/16:0, PC 18:1/18:1, PC 16:0/18:1, PC 18:1/16:0, ECN 32) and polyunsaturated phosphatidylcholines (PC 16:0/18:2, ECN 30; PC 16:0/20:4, PC 18:2/18:2, ECN 28; PC 20:5/20:5, ECN 20). Values (% area) of PL and FC measured in control and treated HeLa cells (B). Results were expressed as a mean ± standard deviation (SD) of three independent experiments; a = $p < 0.001$ versus Ctrl.

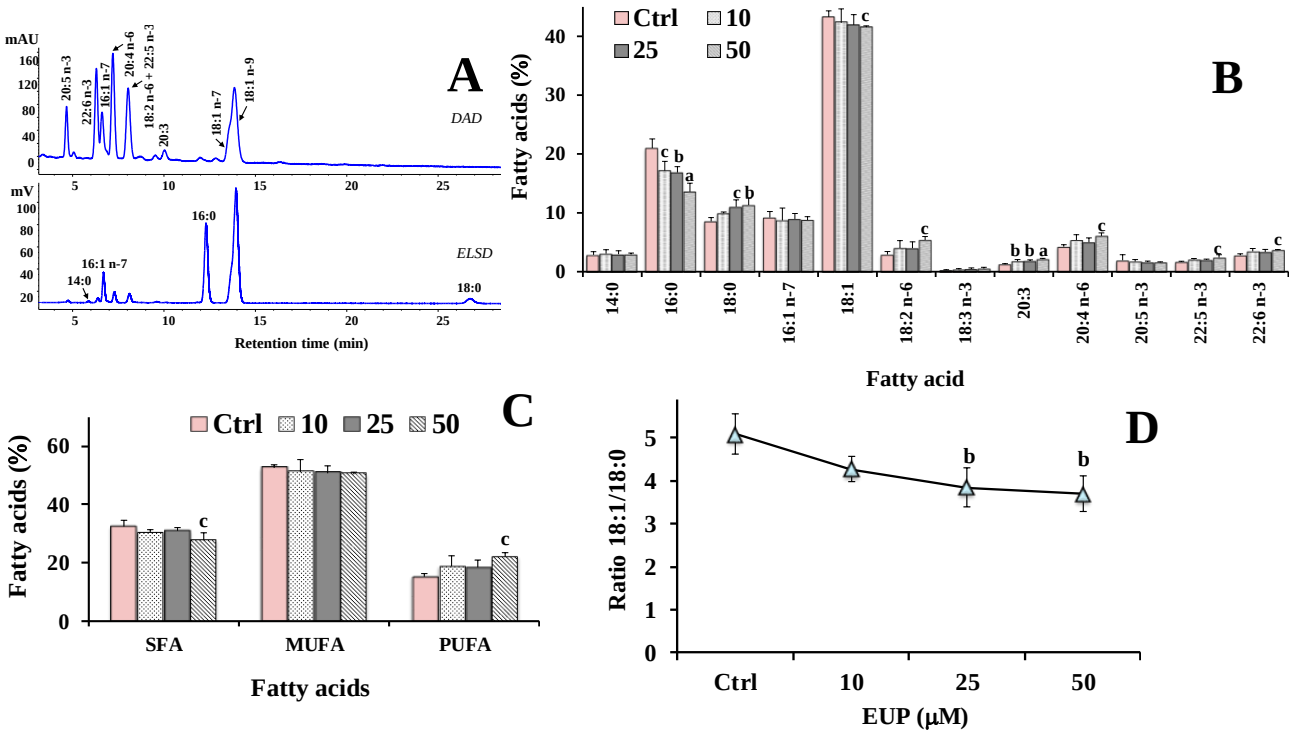

Fig. 6 Fatty acid chromatographic profile of control HeLa cells (Ctrl) obtained by HPLC analysis with DAD (at 200 nm) and ELSD detection (A). Values (expressed as % of total fatty acids) of the main fatty acids (B), total saturated (SFA), monounsaturated (MUFA) and polyunsaturated (PUFA) fatty acids (C), and values of the ratios 18:1 n-9/18:0 (D) measured in HeLa control cells and cells treated for 24 h with eupatilin (EUP) 10, 25 and 50 μM. Three independent experiments and two replicates for each condition are performed and data are presented as mean ± SD (n = 6), a = $p < 0.001$, b = $p < 0.01$, c = $p < 0.05$ versus Ctrl.

modulation of the total cancer cell lipid profile.

Fig. 6A shows the representative FA chromatographic profile of HeLa control cells obtained by HPLC-DAD/ELSD analysis. HeLa control cells showed a FA composition (Fig. 6B and 6C) characterized by a high level of 18:1 isomers (130.2 ± 23.2 μg/plate, 43% of TFA; mainly 18:1 n-9), 16:0 (63.1 ± 11.9 μg/plate, 21%), stearic acid 18:0 (25.5 ± 2.8 μg/plate, 9%), and palmitoleic acid 16:1 n-7 (27.4 ± 3.2 μg/plate, 9%), while 20:4 n-6 (12.8 ± 2.8 μg/plate, 4%) represented the most abundant FA among polyunsaturated FA (PUFA). Values of FA (expressed as % of TFA) measured in HeLa cells after 24 h of incubation in the presence of EUP (10, 25 and 50 μM) are reported in Figs. 6B and 6C. The incubation of cancer HeLa cells with EUP induced marked changes in the FA profile with respect to untreated-control cells from the lowest tested dose (10 μM). The incubation of HeLa cells with EUP induced a dose-dependent decrease in the % cell level of SFA and MUFA, coupled to the increase of PUFA % value (Fig. 6C). Interestingly, EUP treatment induced a marked significant reduction in the levels of 16:0 at all tested doses (at EUP 50 μM: 13% of total fatty acids, $p < 0.001$ versus control cells) together with a % increase in the level of 18:0 and the decrease of 18:1 n-9 cell amount. The 18:1 n-9/18:0 ratio value (Fig. 6D) noticeably decreased in EUP-treated cells at all tested concentrations with respect to untreated-control cells characterized by the value of 5.1 ± 0.5), and values of 3.8 ± 0.5 ($p < 0.01$) and 3.7 ± 0.4 ($p < 0.01$) were determined in 25 μM and 50 μM-ZER treated cells, respectively. Moreover EUP, at all tested doses, did not affect the levels of the oxidative products HP, in comparison to control cells (data not shown), excluding an evident lipid peroxidation process. Cell treated with DMSO, used to dissolve the compound, did not show differences in the FA levels with respect to controls.

3.5. Apoptosis induction in HeLa cells

To evaluate the apoptosis induced by the EUP treatment, HeLa cells were stained by Annexin V and PI. Cells were scored as early apoptotic (green) or late apoptotic (green-red) based on Annexin V-positive staining only, or both Annexin V and PI positivity, respectively. Viable cells were scored by the absence of Annexin V and PI staining. The immunofluorescence staining (Fig. 7A) showed that control cells were negative for staining, whereas EUP (10, 25, and 50 μM) induced an increase of the number of early apoptotic cells (rounded and green cells) in concentration-dependent manner. A slight, but non-significant, increase was observed in the number of late apoptotic cells with increasing EUP concentration. The same pattern was observed by the cytometric analysis (Fig. 7B). Fig. 7C shows the total percentage of apoptotic EUP-treated cells (10, 25, and 50 μM) compared to control cells, while the % proportion of early apoptotic and late apoptotic treated cells compared to control cells is reported in Fig. 7D. The highest % of apoptotic cells was observed in HeLa cells treated with EUP 50 μM (Fig. 7C), characterized by a prevalent amount of early apoptotic cells (20%) (Fig. 7D). The presence of necrotic cells was not significantly different between treated and control cells (data not shown). Moreover, the immunofluorescence staining showed the presence a great number of non-apoptotic rounded cells, indicative of an intense mitotic process.

3.6. Effect on cell membranes, nuclei, and mitochondrial potential

Phase contrast and NR fluorescence images (Fig. 8) show that control HeLa cells were small, packed and mononucleated with a bright fluorescence corresponding to their inner cell membranes. Confirming observations with Annexin V and PI, treatment with various EUP doses elicited the occurrence of reduced volume apoptotic cells, which dramatically increased in number, following the doses of 25 and 50 μM. In these conditions, the other non-apoptotic cells were able to spread widely because of the increased free surface. These “spread” cells did not show main changes in cell membranes

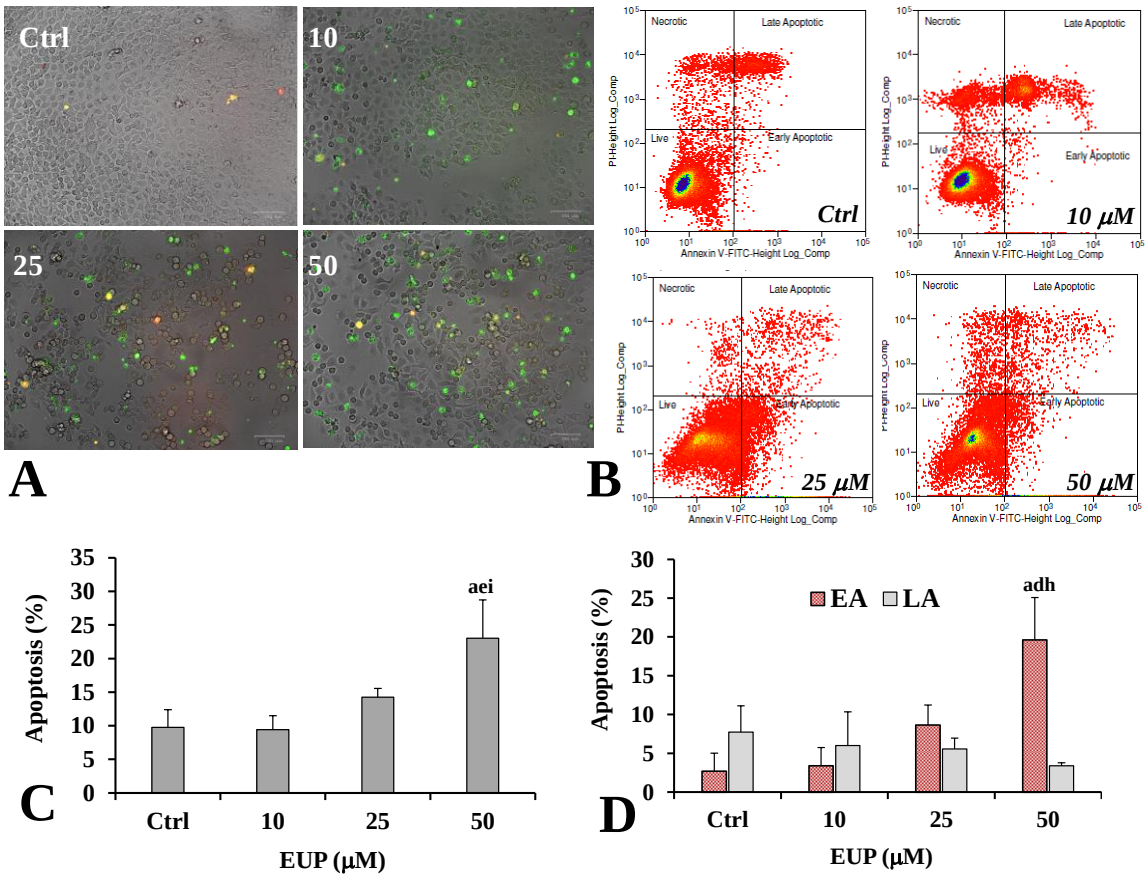

Fig. 7 Merged images of the brightfield, red and green fluorescence channels. Early apoptotic cells were stained by Alexa Fluor 488 Annexin V (green), late apoptotic cells were stained by Annexin V and PI (green-red) staining after 24 h of treatment with eupatilin (EUP) (10, 25, 50 μM) (A). Different distribution of HeLa cells stained with Annexin V-FITC/PI in a dual parametric dot plots of PI fluorescence (Y-axis) versus Annexin V-FITC fluorescence (X-axis) (B). Total percentage of apoptotic cells (C) and the proportion of early apoptotic and late apoptotic cells (D) measured in control cells (Ctrl) and cells treated for 24 h with EUP (10, 25 or 50 μM). Values are expressed as mean ± SD obtained from at least three independent experiments; (n = 9); a = $p < 0.001$ versus Ctrl; d = $p < 0.001$, e = $p < 0.01$ versus 10 μM; h = $p < 0.01$, i = $p < 0.05$ versus 25 μM.

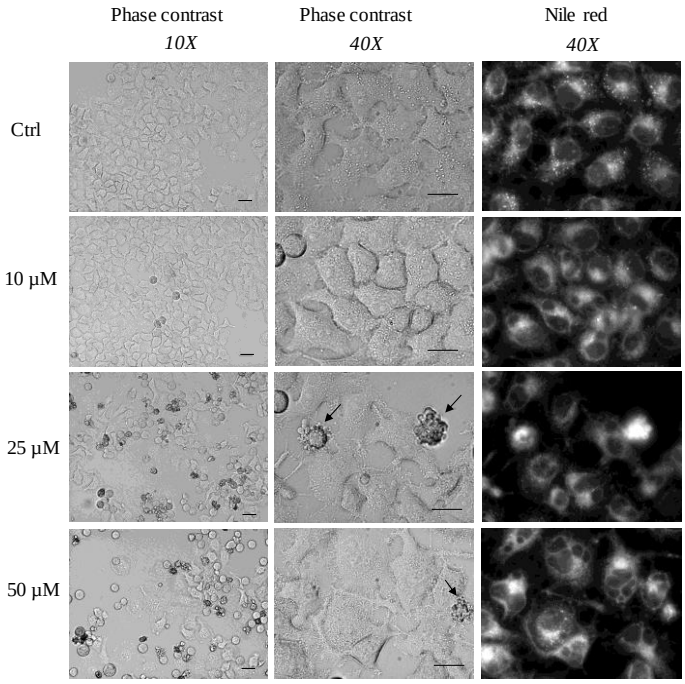

Fig. 8 Representative images of HeLa cells by phase contrast and fluorescence microscopy observation. Control cells (Ctrl) and cells treated for 24 h with 10, 25 or 50 µM EUP were stained with Nile Red (NR) and their red emission was acquired as corresponding to cell membranes. Arrows indicate apoptotic bodies. Bar = 50 µm.

fluorescence (NR, red emission), but displayed multiple nuclei, which were more frequently observed at the higher EUP concentrations, discernible both in phase contrast, NR- and DAPI-stained cells (Fig. 8 and Fig. 9A). Moreover, despite the occurrence of clear apoptotic bodies, mitotic figures were always observed even at the highest EUP concentrations (Fig. 9B).

Mitochondrial potential underwent a decrease of about 40% after 10 µM EUP treatment (Fig. 9C). The reduction in mitochondrial potential was similar for every tested concentration of EUP. Mitochondrial morphology displayed a regular mitochondrial network in control cells, in which mitochondria were regularly thick. Higher EUP concentrations did not reveal changes in mitochondrial morphology, which maintained the appearance as a network with normally thickened mitochondria. When apoptotic bodies were visualized (Fig. 9), they displayed no mitochondrial potential. Hence, the morphology here described as mitochondrial was referred to "spread cells", which maintained the appearance of "normal" cells, except for the intensity of the mitochondrial potential and, often, of the nuclei's number.

4. Discussion

Dietary flavonoids are thought to have health-promoting properties due to their high antioxidant capacity both *in vivo* and *in vitro* systems.[22] They play a decisive role in protecting various cell types from oxidative stress via different mechanisms. Most of them are bifunctional antioxidants because exert their antioxidant action directly, by scavenging of reactive oxygen species (ROS), and indirectly, by inducing cytoprotective enzymes and transcriptional genes with

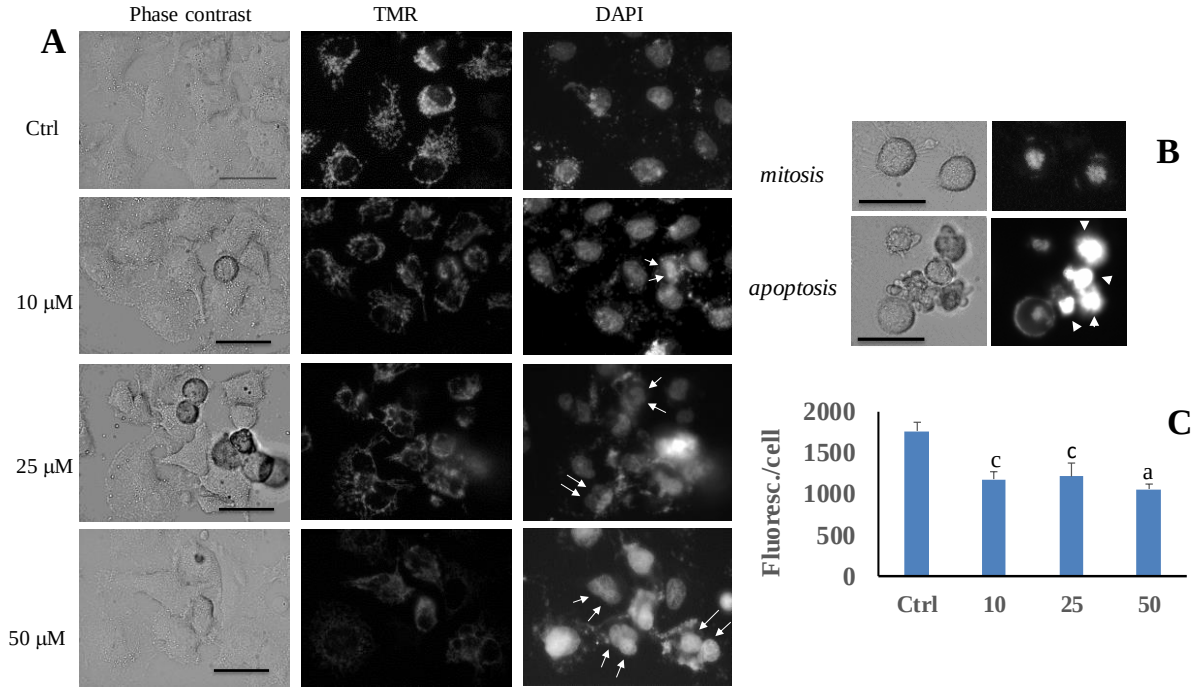

Fig. 9 Phase contrast, mitochondrial potential and nuclear stain as revealed by TMRM and DAPI fluorescence, respectively, on HeLa cells. Mitochondria potential and nuclear fluorescence after eupatilin (EUP) treatment (10, 25 and 50 µM) (A). Mitotic and apoptotic figures after 50 µM EUP for 24 h (B) and the mitochondrial potential variations after EUP as resulted after image analysis (C). EUP treatment decreased mitochondrial potential in each tested dose. Data are expressed as fluorescence intensity per cell and SEM. Arrows display multiple nuclei; arrowheads indicate picnotic nuclei Bar = 50 µm. a = $p < 0.001$, c = $p < 0.05$ versus controls (Ctrl).

antioxidant properties that ensure long-term protection.[22,42] Data from *in vitro* studies have shown that the flavonoid direct antioxidant activity depends upon mechanisms of radical scavenging and metal ion chelation.[22] The configuration, substitution, and total number of hydroxyl groups substantially influence the antioxidant potency of flavonoids and the B ring hydroxyl configuration has been indicated as the most significant determinant of the free radical scavenging action donating hydrogen and an electron to free radicals, stabilizing them.[22] Some studies raised the possibility that also the indirect (induction of antioxidant enzymes) antioxidant activities of flavonoids is determined by the extent and nature of their hydroxylation.[42]

The dietary flavone EUP has been reported to be effective in protecting cells and tissues from ROS in different oxidative stress systems by promoting an indirect antioxidant effect, possibly through the enhancement of the cellular antioxidant pathway,[1,8,14,15] however, few studies reported the direct scavenging activity of EUP toward ROS.[14,17,18] In this study we evaluated the direct antioxidant activity of EUP to prevent lipid degradation in oxidative stress systems of biological relevance, like the oxidative damage to cholesterol, and liposome membranes, *in vitro* models amply validated on natural compounds.[34,37,40,41] Cholesterol is an essential component of biological membranes and lipoproteins and its oxidative products, oxysterols, possess pro-oxidative and pro-inflammatory properties that can play a role in the development of tissue damage associated with pathological events and finally contribute to carcinogenesis.[43] In our cholesterol oxidation assay, the protective effect of an antioxidant is due to a lipoperoxyl (LOO•) radical scavenging activity, strictly correlated to the presence of hydrogen donating substituents like phenolic hydroxyl groups; in addition, lipophilicity, thermal stability, steric hindrance, and volatility of the tested compound have been shown to affect the antioxidant potency.[34,37,40,41] In this system EUP, although less potent than the reference compound QRC, showed an interesting antioxidant protection against cholesterol degradation, comparable to that of the bioactive phenolic compounds arzanol, methylarzanol, and prenylcurcumin.[34,40] The LOO• radical scavenging properties of EUP could be correlated to its ability to donate H-atom from the phenolic functional group (ring A), acting as chain-breaking antioxidant. The reference compound QRC is the most famous antioxidant flavonoid, bearing a catechol moiety (ring B) linked in position 2 to the polyhydroxylated chromen-4-one core. Its strong LOO• radical scavenging activity has been previously demonstrated and the catechol ring B is the "active" moiety, trapping LOO• radicals by formal H-atom transfer (the mechanism described as a concerted electron–proton transfer, EPT).[44]

Liposomes are considered an important membrane model, and numerous studies have been carried out to understand the role of lipid oxidation in phospholipid membranes to prevent, modulate, and treat their oxidative damage.[45] EUP showed the ability to protect liposomes against copper-induced oxidation at 37 °C. The antioxidant activity of this flavone in this system could be related again to a direct LOO• scavenging activity, coupled to a Cu^{++} ion chelation ability.[34,37,40,41] Moreover, EUP lipophilicity could significantly contribute to the antioxidant potency, affecting the flavone interaction with the phospholipid bilayer.[46] As expected, the reference compound QRC in this oxidative assay showed more potency compared to EUP, due to its well-known powerful LOO• scavenging activity in water systems coupled to its iron-chelating and iron-stabilizing properties.[22,44] A large body of evidence suggests that oxidative stress and its associated lipid peroxidation are involved in atherosclerosis, cancer, inflammation and neurodegenerative diseases[31] and the anti-inflammatory and antitumor activity of many natural drugs has been reported to be also mediated through their antioxidant activity and their ability to prevent lipid peroxidation.[22,31,32] Our results showed that EUP is a direct inhibitor of lipid peroxidation in biological *in vitro* systems, validating its potential role as antioxidant agent for the treatment/prevention of disorders implicating a membrane lipid oxidative damage.

One of the most important metabolic hallmarks of cancer cells is deregulation of lipid metabolism.[25-27,47] Cancer cells show specific alterations in different aspects of lipid metabolism (fatty-acid biosynthesis and desaturation, phospholipids and cholesterol metabolism, lipid droplet synthesis).[25-27,47] Therefore, targeting lipid metabolism is a promising therapeutic strategy for human cancer.[25,29] The antitumor property of EUP has been associated to its ability to modulate a variety of signaling pathways and molecular targets in different cancer cell types,[1] disrupting the cytoskeletal structure,[23] inducing cytotoxic and antiproliferative effects,[3,5,18,19,23] cell circle arrest (at G2/M or at the G1/S),[3,23] apoptosis,[5,19,20] and alterations of the mitochondrial inner membrane potential.[1] We studied, for the first time, the impact of this natural dietary compound, after 24 h of incubation, on cell lipids in cancer HeLa cells, a cell line derived from a human cervical epithelioid carcinoma, widely used as a model for oncological studies.[5,37] That time of incubation was chosen in order to study the EUP effect at a low level of drug cytotoxicity. Anyway, EUP, after 24 h-incubation, significantly reduced viability in cancer HeLa cells in a dose-dependent manner, and cytotoxicity values (30-40% of viability reduction in the dose range 25-200 μM) were comparable to those previously observed in human endometrial cancer Hec1A cells[3] after 48 h of incubation with EUP, but lower than values reported for EUP-treated HeLa cells after 48 h-incubation.[5] In our experimental conditions the well-known antitumor compound QRC[22,48] showed in HeLa cells, at the highest tested doses (50-200 μM), similar cytotoxicity pattern.

Marked changes in cellular lipid composition (PL, FC and total FA profile) were observed in human carcinoma HeLa cells when exposed to 24 h-treatment with EUP and this effect was evident from the lowest tested concentration (10 μM, 89% of viability). The treatment with the flavone significantly modulated HeLa cell lipid profile, with a marked modification in the FA composition (% reduction of 16:0 and 18:1 n-9 and accumulation of 18:0) and PL (decrease in the % of S/M-PL). Phosphatidylcholines (PC) represent the predominant polar lipid class (53%) in HeLa cell membranes and the dominant PC in the HeLa cells are PC 16:0/18:1 (approx. 28%), PC18:1/18:1 (approx. 15%), PC16:0/16:1 (approx. 6%).[37,49] The EUP-induced marked decrease in the peak area of S/M-PL could therefore be ascribable to the reduction of PL containing 18:1 n-9 and 16:0. The reduction of palmitic acid was compatible with a potential EUP-induced abrogation of lipid synthesis. Fatty acid synthase (FAS) is a multi-enzyme that catalyzes de novo palmitic acid synthesis, using acetyl-CoA and malonyl-CoA as

substrate[26,29,30] and many anticancer drugs are FAS inhibitors.[26,29] Cancer cells treated with FAS inhibitors are found to undergo apoptosis both *in vitro* and *in vivo* and several flavonoids are reported to inhibit FAS, among them lutein, quercetin and amentoflavone.[29] The reduction of 18:1 n-9 and the accumulation of 18:0 observed in EUP-treated HeLa cells were compatible with a potential EUP-induced inhibition of the enzyme stearoyl-CoA desaturase (SCD). SCD, that inserts a double bond in the Δ^9 position of SFA to generate monounsaturated MUFA, is an effective cancer target.[26,30,47,50] The main product of SCD, oleic acid, provides key substrates for the generation of complex lipids such as phospholipids, triglycerides and cholesterol esters.[26] Small molecules that inhibit SCD are toxic to cancer cell lines because these cells often require de novo synthesis of UFA to generate membranes and maintain membrane fluidity, essential to cell proliferation.[25,47,50] Therefore, inhibition of SCD leads to UFA depletion and cell death, influences the phospholipid composition of cellular membranes, and thus affects membrane properties.[50] EUP showed in cancer HeLa cells the ability to modulate the FA profile, maybe reducing lipogenesis and affecting FA desaturation, and the biosynthesis of PL, that represent building blocks for biological membranes. In cancer cells, changes in lipid components severely affect functional and biophysical properties of cytoplasmic and organelle membranes (changes in membrane organization, structure and fluidity), perturbing membrane lipid raft and protein dynamics and inducing apoptotic pathways. [25,28,47,50]

Apoptosis appearance and changes occurring on cytoplasmic membranes, nuclear morphology and mitochondria membrane potential were also investigated in EUP-treated cancer cells. Apoptotic cell death is a common and important phenomenon for various anticancer drugs and several lines of evidence suggest that the induction of apoptosis is one of the major mechanisms underlying the anti-proliferative activity of EUP, as observed in many tumor cell lines.[1,5] The reported pro-apoptotic activity of EUP on cancer cells has been related to an increase of ROS production[1,20] and the activation/inhibition of numerous signaling pathways.[1,3,5,18-20] A recent study evidenced the EUP ability to inhibit proliferation in cervical cancer cell lines (HeLa and Caski) via promoting apoptosis and cell cycle arrest (G0/G1 phase arrest) and by inhibiting the hedgehog signal pathway.[5] In our experimental conditions, flow cytometry, immunofluorescence and fluorescence microscopy evidenced the EUP ability to induce early stages of apoptosis (round reduced volume cells, membrane blebbing, and formation of apoptotic bodies) and to alter the nuclear morphology of HeLa cancer cells. After 24 h of incubation, the highest % of apoptotic cells was observed with EUP 50 μM (20%) and this value was comparable to that previously observed in cancer HeLa cells treated for 48 h with EUP 40 μM and stained with Hoechst.[5] In addition to apoptotic cells, EUP induced, after 24-incubation, the growth of HeLa cells with multiple nuclei as index of an abnormal mitosis. Mitotic catastrophe (MC) is a type of cell death due to abnormal mitotic events that produce spontaneous premature chromosome condensation and cell division with the characteristic features of polynucleated cells.[51,52] MC is accompanied by micronucleation resulting from chromosome fragments and multinucleation presenting two or more nuclei residues from a deficient separation during cytokinesis.[52] MC causes a delayed mitosis-linked cell death and finally leads to apoptosis and it is involved in the effects of several anticancer extracts/compounds, as well (apple polyphenols, imidazoacridinone C-1311 and yessotoxin).[51-53] Since mitochondria are a common target of apoptotic stimuli, the anticancer activity of EUP has also been previously associated to a mitochondrial dysfunction.[1] Moreover, according to literature,[1] our data disclosed a significant decrease of the mitochondrial membrane potential after 24-h incubation of HeLa cells from the lowest dose of EUP. Changes in the mitochondrial membrane potential are a major adaptation process to a variety of environmental factors that regulate increased energy demands, cell growth and differentiation or cellular stress,[37] but they also occur during apoptosis, that can be triggered by extracellular signals or by intracellular events related to cellular stress. The reduction in mitochondrial potential (observed in "spread cells") was similar at all EUP concentrations, however the phenol did not induced changes in mitochondrial morphology.

We presented evidences that EUP induced cytotoxicity, apoptosis and abnormal mitosis, affecting lipid profile and mitochondrial potential in cancer HeLa cells. In our study, the EUP effects were strictly correlated with the dose. The 24-h incubation of HeLa cells with the lowest concentration of EUP (10 μM) induced a reduction of viability (11%), marked changes in PL and FA profile, an abnormal mitosis (formation of "spread" cells with multiple nuclei), and mitochondrial depolarization, with low level of early apoptotic cells. The treatment with EUP 25 and 50 μM induced significant cytotoxicity, marked changes in lipid profile and mitochondrial depolarization, dramatically increasing the number of round non-apoptotic (mitotic cells) and apoptotic cells (early apoptosis) that appeared together with multinucleated cells. Thus, EUP significantly affected the metabolic functions of cancer HeLa cells acting simultaneously through different mechanisms, however it was very difficult to assess the exact sequence of action of this dietary compound.

5. Conclusions

Taken together, our results validate the EUP role as antioxidant agent for the treatment/prevention of disorders implicating a membrane lipid oxidative damage and for the first time substantiate lipid metabolism as another possible biological target of this dietary natural flavonoid in cancer HeLa cells. Further studies are needed to explore the EUP lipid targeting mechanism in cancer and normal cells.

Conflicts of interest

There are no conflicts to declare.

Acknowledgements

This work was supported by the Research Integrative Fund of the University of Cagliari to MN. We acknowledge the CeSAR (Centro Servizi Ricerca d'Ateneo) core facility of the University of Cagliari and Dr. Rita Pillai for assistance with the generation of Flow Cytometry data.

References

1 B. Nageen, I. Sarfraz, A. Rasul, G. Hussain, F. Rukhsar, S. Irshad, A. Riaz, Z. Selamoglu and M. Ali, Eupatilin: a natural pharmacologically active flavone compound with its wide range applications*, J. Asian Nat. Prod. Res.*, 2020, **22**, 1-16.

2 B. Ivănescu, C. Tuchiluş, A. Corciovă, C. Lungu, C. T. Mihai, A.-M. Gheldiu and L. Vlase, Antioxidant, antimicrobial and cytotoxic activity of *Tanacetum vulgare*, *Tanacetum corymbosum* and *Tanacetum macrophyllum* extracts, *Farmacia*, 2018, **66**, 282-288.

3 J. H. Cho, J. G. Lee, Y. I. Yang, J. H. Kim, J. H. Ahn, N. I. Baek, K. T. Lee and J. H. Choi, Eupatilin, a dietary flavonoid, induces G2/M cell cycle arrest in human endometrial cancer cells, *Food Chem. Toxicol.*, 2011, **49**, 1737-1744.

4 A. Giangaspero, C. Ponti, F. Pollastro, G. Del Favero, R. Della Loggia, A. Tubaro, G. Appendino and S. Sosa, Topical anti-inflammatory activity of eupatilin, a lipophilic flavonoid from mountain wormwood (*Artemisia umbelliformis* Lam.), *J. Agric. Food Chem.*, 2009, **57**, 7726-7730.

5 Z. Wu, B. Zou, X. Zhang and X. Peng, Eupatilin regulates proliferation and cell cycle of cervical cancer by regulating hedgehog signalling pathway, *Cell Biochem. Funct.*, 2020, in press, DOI: 10.1002/cbf.3493.

6 J. F. Vouillamoz, C. Carlen, O. Taglialatela-Scafati, F. Pollastro and G. Appendino, The génépi Artemisia species. Ethnopharmacology, cultivation, phytochemistry, and bioactivity, *Fitoterapia*, 2015, **106**, 231-241.

7 Y. Jung, J. C. Kim, Y. Choi, S. Lee, K. S. Kang, Y. K. Kim and S. N. Kim, Eupatilin with PPARα agonistic effects inhibits TNFα-induced MMP signaling in HaCaT cells, *Biochem. Biophys. Res. Commun.*, 2017, **493**, 220-226.

8 K. Zhou, R. Cheng, B. Liu, L. Wang, H. Xie and C. Zhang, Eupatilin ameliorates dextran sulphate sodium-induced colitis in mice partly through promoting AMPK activation, *Phytomedicine*, 2018, **46**, 46-56.

9 Y. D. Kim, S. C. Choi, T. Y. Oh, J. S. Chun, and C. D. Jun, Eupatilin inhibits T-cell activation by modulation of intracellular calcium flux and NF-κB and NF-AT activity, *J. Cell Biochem.*, 2009, **108**, 225-236.

10 Z. Qiao, Y. W. Xu and J. Yang, Eupatilin inhibits the apoptosis in H9c2 cardiomyocytes via the Akt/GSK-3β pathway following hypoxia/reoxygenation injury, *Biomed Pharmacother.*, 2016, **82**, 373-378.

11 E. H. Song, K. S. Chung, Y. M. Kang, J. H. Lee, M. Lee and H. J. An, Eupatilin suppresses the allergic inflammatory response *in vitro* and *in vivo*, *Phytomedicine*, 2018, **42**, 1-8.

12 J. S. Kim, S. G. Lee, K. Min, T. K. Kwon, H. J. Kim and J. O. Nam, Eupatilin inhibits adipogenesis through suppression of PPAR? activity in 3T3-L1 cells, *Biomed Pharmacother.*, 2018, **103**, 135-139.

13 A. Sapkota, B. P. Gaire, K. S. Cho, S. J. Jeon, O. W. Kwon, D. S. Jang, S. Y. Kim, J. H. Ryu and J. W. Choi, Eupatilin exerts neuroprotective effects in mice with transient focal cerebral ischemia by reducing microglial activation, *PLoS One*, 2017, **12**, e0171479.

14 Choi, E. J., Oh, H. M., Na, B. R., Ramesh, T. P., Lee, H. J., Choi, C. S., S. C. Choi, T. Y. Oh, S. J. Choi, J. R. Chae, S. W. Kim and C. D. Jun, Eupatilin protects gastric epithelial cells from oxidative damage and down-regulates genes responsible for the cellular oxidative stress, *Pharm. Res.*, 2008, **25**, 1355-1364.

15 L. Du, J. Chen and Y. Q. Xing, Eupatilin prevents H_2O_2-induced oxidative stress and apoptosis in human retinal pigment epithelial cells, *Biomed. Pharmacother.*, 2017, **85**, 136-140.

16 J. H. Jeong, S. J. Moon, J. Y. Jhun, E. J. Yang, M. L. Cho and J. K. Min, Eupatilin exerts antinociceptive and chondroprotective properties in a rat model of osteoarthritis by downregulating oxidative damage and catabolic activity in chondrocytes, *PLoS One*, 2015, **10**, e0130882.

17 M. Li, W. Liu, C. Peng, Q. Ren, W. Lu, and W. Deng, A DFT study on reaction of eupatilin with hydroxyl radical in solution. *Int. J. Quantum Chem.*, 2013, **113**, 966-974.

18 J. Y. Park, D. Lee, H. J. Jang, D. S. Jang, H. C. Kwon, K. H. Kim, S. N. Kim, G. S. Hwang, K. S. Kang and D. W. Eom, Protective effect of *Artemisia asiatica* extract and its active compound eupatilin against cisplatin-induced renal damage, *Evid. Based Complement. Alternat. Med.*, 2015, **2015**, 483980.

19 Y. Wang, H. Hou, M. Li, Y. Yang and L. Sun, Anticancer effect of eupatilin on glioma cells through inhibition of the Notch-1 signaling pathway, *Mol. Med. Rep.*, 2016, **13**, 1141-1146.

20 W. F. Zhong, X. H. Wang, B. Pan, F. Li, L. Kuang and Z. X. Su, Eupatilin induces human renal cancer cell apoptosis via ROS-mediated MAPK and PI3K/AKT signaling pathways, *Oncol Lett.*, 2016, **12**, 2894-2899.

21 S. B. Ryoo, H. K. Oh, S. A. Yu, S. H. Moon, E. K. Choe, T. Y. Oh and K. J. Park, The effects of eupatilin (stillen®) on motility of human lower gastrointestinal tracts, *Korean J. Physiol. Pharmacol.*, 2014, **18**, 383-390.

22 S. Kumar and A. K. Pandey, Chemistry and biological activities of flavonoids: an overview, *ScientificWorldJournal*, 2013, **29**, 162750.

23 X. Fei, J. Wang, C. Chen, B. Ding, X. Fu, W. Chen, C. Wang and R. Xu, Eupatilin inhibits glioma proliferation, migration, and invasion by arresting cell cycle at G1/S phase and disrupting the cytoskeletal structure, *Cancer Manag. Res.*, 2019, **11**, 4781-4796.

24 J. Y. Park, D. H. Park, Y. Jeon, Y. J. Kim, J. Lee, M. S. Shin, K. S. Kang, G. S. Hwang and H. Y. Kim, Eupatilin inhibits angiogenesis-mediated human hepatocellular metastasis by reducing MMP-2 and VEGF signaling, *Bioorg. Med. Chem. Lett.*, 2018, **28**, 3150-3154.

25 Q. Liu, Q. Luo, A. Halim and G. Song, Targeting lipid metabolism of cancer cells: A promising therapeutic strategy for cancer, *Cancer Lett.*, 2017, **401**, 39–45.

26 X. Luo, C. Cheng, Z. Tan, N. Li, M. Tang, L. Yang and Y. Cao, Emerging roles of lipid metabolism in cancer metastasis, *Mol. Cancer.*, 2017, **16**, 76.

27 A. Pakiet, J. Kobiela, P. Stepnowski, T. Sledzinski, and A. Mika, Changes in lipids composition and metabolism in colorectal cancer: a review, *Lipids Health Dis.*, 2019, **18**, 29.

28 V. Lladó, D. J. López, M. Ibarguren, M. Alonso, J. B. Soriano, P. V. Escribá and X. Busquets, Regulation of the cancer cell membrane lipid composition by NaCHOleate. Effects on cell signaling and therapeutical relevance in glioma, *Biochim. Biophys. Acta,* 2014, **1838**, 1619-1627.

29 J. S. Zhang, J. P. Lei, G. Q. Wei, H. Chen, C. Y. Ma and H. Z. Jiang, Natural fatty acid synthase inhibitors as potent therapeutic agents for cancers: A review, *Pharm. Biol.*, 2016, **54**, 1919-1925.

30 V. Fritz, Z. Benfodda, C. Henriquet, S. Hure, J. P. Cristol, F. Michel, M. A. Carbonneau, F. Casas and L. Fajas, Metabolic intervention on lipid synthesis converging pathways abrogates prostate cancer growth, *Oncogene*, 2013, **32**, 5101-5110.

31 G. Barrera, Oxidative stress and lipid peroxidation products in cancer progression and therapy, *ISRN Oncol.*, 2012, **2012**, 137289.

32 B. L. Tan, M. E. Norhaizan, W. P. Liew and H. Sulaiman Rahman, Antioxidant and oxidative stress: a mutual interplay in age-related diseases, *Front. Pharmacol.*, 2018, **16**, 1162.

33 G. Appendino, O. Taglialatela-Scafati, A. Romano, F. Pollastro, C. Avonto and P. Rubiolo, Genepolide, a sesterpene-γ-lactone with a novel carbon skeleton from mountain wormwood (*Artemisia umbelliformis*), *J. Nat. Prod.*, 2009, **73**, 340-344.

34 A. Rosa, A. Atzeri, M. Nieddu and G. Appendino, New insights into the antioxidant activity and cytotoxicity of arzanol and

effect of methylation on its biological properties, *Chem. Phys. Lipids*, 2017, **205**, 55-64.
35 A. Rosa, P. Scano, A. Atzeri, M. Deiana and A. M. Falchi, Potential anti-tumor effects of *Mugil cephalus* processed roe extracts on colon cancer cells, *Food Chem. Toxicol.*, 2013, **60**, 471-478.
36 A. Rosa, A. Piras, M. Nieddu, D. Putzu, F. Cesare Marincola and A. M. Falchi, *Mugil cephalus* roe oil obtained by supercritical fluid extraction affects lipid profile and viability in cancer HeLa and B16F10 cells, *Food Funct.*, 2016, **7**, 4092-4103.
37 A. Rosa, D. Caprioglio, R. Isola, M. Nieddu, G. Appendino and A. M. Falchi, Dietary zerumbone from shampoo ginger: new insights into its antioxidant and anticancer activity, *Food Funct.*, 2019, **10**, 1629-1642.
38 A. M. Falchi, R. Isola, A. Diana, M. Putzolu and G. Diaz, Characterization of depolarization and repolarization phases of mitochondrial membrane potential fluctuations induced by tetramethylrhodamine methyl ester photoactivation, *FEBS J.*, 2005, **272**, 1649-1659.
39 R. Isola, P. Solinas, F. Loy, S. Mariotti and A. Riva, 3-D structure of mitochondrial cristae in rat adrenal cortex varies after acute stimulation with ACTH and CRH, *Mitochondrion*, 2010, **10**, 472-478.
40 A. Rosa, A. Atzeri, M. Deiana, M. P. Melis, A. Incani, A. Minassi, B. Cabboi and G. Appendino, Prenylation preserves antioxidant properties and effect on cell viability of the natural dietary phenol curcumin, *Food Res. Int.*, 2014, **57**, 225–233.
41 A. Rosa, C. I. Tuberoso, A. Atzeri, M. P. Melis, E. Bifulco and M. A. Dessì, Antioxidant profile of strawberry tree honey and its marker homogentisic acid in several models of oxidative stress, *Food Chem.*, 2011, **129**, 1045-1053.
42 B. Sengupta, M. Sahihi, M. Dehkhodaei, D. Kelly and I. Arany, Differential roles of 3-hydroxyflavone and 7-hydroxyflavone against nicotine-induced oxidative stress in rat renal proximal tubule cells, *PLoS One*, 2017, **12**, e0179777.
43 C. Garenc, P. Julien and E. Levy, Oxysterols in biological systems: the gastrointestinal tract, liver, vascular wall and central nervous system, *Free Rad. Res.*, 2010, **44**, 47-73.
44 R. Amorati, A. Baschieri, A. Cowden and L. Valgimigli, The antioxidant activity of quercetin in water solution, *Biomimetics (Basel)*, 2017, **2**, 9.
45 M. Mosca, A. Ceglie and L. Ambrosone, Effect of membrane composition on lipid oxidation in liposomes, *Chem. Phys. Lipids*, 2011, **164**, 158-165.
46 Y. S. Tarahovsky, Y. A. Kim, E. A. Yagolnik and E. N. Muzafarov, Flavonoid-membrane interactions: involvement of flavonoid-metal complexes in raft signaling, *Biochim. Biophys. Acta*, 2014, **1838**, 1235-1246.
47 C. R. Santos and A. Schulze, Lipid metabolism in cancer, *FEBS J.*, 2012, **279**, 2610–2623.
48 L. Gibellini, M. Pinti, M. Nasi, J. P. Montagna, S. De Biasi, E. Roat, L. Bertoncelli, E. L. Cooper and A. Cossarizza, Quercetin and cancer chemoprevention, *Evid. Based Complement. Alternat. Med.*, 2011, **2011**, 591356.
49 M. K. Dymond, C. V. Hague, A. D. Postle and G. S. Attard, An in vivo ratio control mechanism for phospholipid homeostasis: evidence from lipidomic studies, *J. R. Soc. Interface*, 2012, **10**, 20120854.
50 P. C. Theodoropoulos, S. S. Gonzales, S. E. Winterton, C. Rodriguez-Navas, J. S. McKnight, L. K. Morlock, J. M. Hanson, B. Cross, A. E. Owen, Y. Duan, J. R. Moreno, A. Lemoff, H. Mirzaei, B. A. Posner, N. S. Williams, J. M. Ready and D. Nijhawan, Discovery of tumor-specific irreversible inhibitors of stearoyl CoA desaturase, *Nat. Chem. Biol.*, 2016, **12**, 218-225.
51 A. Skwarska, E. Augustin and J. Konopa, Sequential induction of mitotic catastrophe followed by apoptosis in human leukemia MOLT4 cells by imidazoacridinone C-1311, *Apoptosis*, 2007, **12**, 2245-2257.
52 Y. L. Kao, Y. M. Kuo, Y. R. Lee, S. F. Yang, W. R. Chen and H. J. Lee, Apple polyphenol induces cell apoptosis, cell cycle arrest at G2/M phase, and mitotic catastrophe in human bladder transitional carcinoma cells, *J. Funct. Foods*, 2015, **14**, 384-394.
53 M. S. Korsnes and R. Korsnes, Mitotic catastrophe in BC3H1 cells following yessotoxin exposure, *Front. Cell Dev. Biol.*, 2017, **5**, 30.